Supplementary material

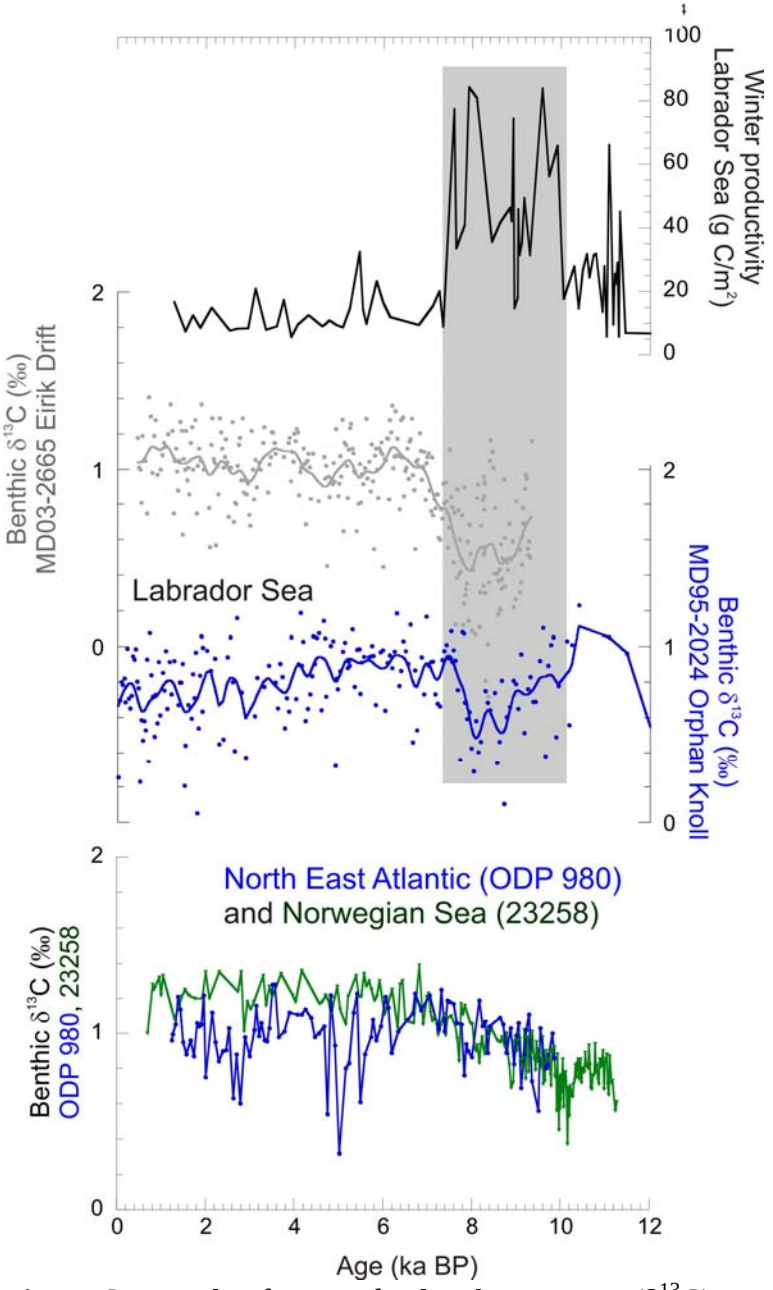

Figure S1. Benthic foraminiferal carbon isotope ($\delta^{13}C$) records from the Labrador Sea (Eirik Drift core MD03-2665 from Kleiven et al. (2008), Orphan Knoll core MD95-2024), North East Atlantic (ODP 980 from Oppo et al., (2003)) and Norwegian Sea (23258 from Sarnthein et al., (2003)), and a Labrador Sea winter productivity record from Radi and de Vernal (2008). An interval of depleted $\delta^{13}C$ between 10 and 7.5 ka is likely caused by increased remineralization of organic material due to increased wintertime productivity.

Table S1. AMS 14C dates measured on the monospecific planktonic foraminifera *Globigerina bulloides* for the Labrador Sea Site (box core HU-091-045-09 and piston core MD2024) and Gardar Drift Site (MD99-2251). The latter were originally published in Ellison et al. (2006). Conversion to calendar years before present (cal. yrs BP) with CALIB 501 (Stuiver et al., 1993) using marine04 as calibration data set. Mean ages are the arithmetic means of the age ranges given by the program.

	AMS ^{14}C dates							
	Depth (cm)	Dated species	Laboratory code	Age ±1s (^{14}C yr BP)		Age ranges (cal. yr BP)		**Mean age (cal. yr BP)**
HU-091-045-093	**29**	*G. bulloides*	SUERC-9316	2257	±35	1s:	1816-1910	1863
						2s:	1764-1968	1866
HU-091-045-093	**43**	*G. bulloides*	SUERC-9317	2782	±35	1s:	2442-2609	2526
						2s:	2368-2667	2518
MD95-2024	**0.5**	*G. bulloides*	SUERC-4741	1532	±25	1s:	1048-1132	1090
						2s:	998-1168	1083
MD95-2024	**25.5**	*G. bulloides*	SUERC-4742	2017	±26	1s:	1530-1616	1573
						2s:	1510-1677	1594
MD95-2024	**68.5**	*G. bulloides*	SUERC-6937	2803	±26	1s:	2488-2612	2550
						2s:	2434-2681	2558
MD95-2024	**100.5**	*G. bulloides*	SUERC-4744	3745	±23	1s:	3623-3711	3667
						2s:	3578-3778	3678
MD95-2024	**148.5**	*G. bulloides*	SUERC-6938	4242	±26	1s:	4307-4401	4354
						2s:	4242-4424	4333
MD95-2024	**172.5**	*G. bulloides*	SUERC-8257	5248	±26	1s:	5578-5631	5605
						2s:	5561-5680	5621
MD95-2024	**194.5**	*G. bulloides*	SUERC-8258	5550	±26	1s:	5899-5962	5931
						2s:	5871-6003	5937
MD95-2024	**250.5**	*G. bulloides*	SUERC-11346	6981	±35	1s:	7434-7510	7472
						2s:	7417-7552	7485
MD95-2024	**288.5**	*G. bulloides*	SUERC-5553	7921	±30	1s:	8349-8408	8379
						2s:	8316-8453	8385
MD95-2024	**328.5**	*G. bulloides*	SUERC-6940	9043	±30	1s:	9667-9816	9742
						2s:	9603-9884	9744
MD95-2024	**374.5**	*G. bulloides*	SUERC-8259	9468	±31	1s:	10249-10359	10304
						2s:	10222-10416	10319
MD95-2024	**434.5**	*G. bulloides*	SUERC-6941	12081	±42	1s:	13447-13592	13520
						2s:	13402-13663	13533
MD95-2024	**478.5**	*G. bulloides*	SUERC-6942	13440	±47	1s:	15233-15535	15384
						2s:	15121-15729	15425
MD99-2251	**0**	*G. bulloides*	SUERC-3063	991	±21	1s:	548-609	579
						2s:	526-630	578
MD99-2251	**70**	*G. bulloides*	SUERC-3067	1006	±18	1s:	559-618	589
						2s:	537-637	587
MD99-2251	**140**	*G. bulloides*	SUERC-3068	1403	±21	1s:	915-969	942
						2s:	896-1022	959
MD99-2251	**230**	*G. bulloides*	SUERC-3069	1666	±24	1s:	1202-1267	1235
						2s:	1166-1282	1224

MD99-2251	**280**	*G. bulloides*	SUERC-5178	1888	±25	1s:	1389-1478	1434
						2s:	1354-1512	1433
MD99-2251	**354**	*G. bulloides*	SUERC-5179	2094	±23	1s:	1620-1709	1665
						2s:	1581-1768	1675
MD99-2251	**410**	*G. bulloides*	SUERC-3070	2469	±24	1s:	2061-2157	2109
						2s:	2024-2251	2138
MD99-2251	**484**	*G. bulloides*	SUERC-5182	2576	±25	1s:	2210-2307	2259
						2s:	2156-2323	2240
MD99-2251	**560**	*G. bulloides*	SUERC-3071	2995	±24	1s:	2730-2787	2759
						2s:	2714-2833	2774
MD99-2251	**650**	*G. bulloides*	SUERC-5183	3615	±30	1s:	3461-3555	3508
						2s:	3419-3609	3514
MD99-2251	**740**	*G. bulloides*	SUERC-3072	4100	±22	1s:	4095-4190	4143
						2s:	4093-4197	4195
MD99-2251	**800**	*G. bulloides*	SUERC-5184	4386	±22	1s:	4483-4579	4531
						2s:	4428-4621	4525
MD99-2251	**860**	*G. bulloides*	SUERC-3076	4864	±22	1s:	5130-5257	5194
						2s:	5058-5273	5166
MD99-2251	**910**	*G. bulloides*	SUERC-5185	5109	±24	1s:	5445-5227	5336
						2s:	5399-5570	5485
MD99-2251	**944**	*G. bulloides*	SUERC-5186	5385	±28	1s:	5707-5814	5761
						2s:	5659-5859	5759
MD99-2251	**1034**	*G. bulloides*	SUERC-3079	6341	±31	1s:	6754-6854	6804
						2s:	6709-6905	6807
MD99-2251	**1094**	*G. bulloides*	SUERC-5188	6567	±27	1s:	7046-7146	7096
						2s:	6984-7171	7078
MD99-2251	**1168**	*G. bulloides*	SUERC-5189	7340	±26	1s:	7763-7847	7805
						2s:	7720-7900	7810
MD99-2251	**1220**	*G. bulloides*	SUERC-5192	7815	±35	1s:	8241-8339	8290
						2s:	8187-8362	8275
MD99-2251	**1284**	*G. bulloides*	SUERC-3082	8474	±27	1s:	9017-9124	9071
						2s:	8995-9209	9102
MD99-2251	**1364**	*G. bulloides*	SUERC-3086	8868	±30	1s:	9483-9538	9511
						2s:	9455-9596	9526
MD99-2251	**1474**	*G. bulloides*	SUERC-3087	9365	±34	1s:	10173-10231	10202
						2s:	10139-10285	10212
MD99-2251	**1534**	*G. bulloides*	SUERC-5193	9737	±31	1s:	10545-10614	10580
						2s:	10520-10671	10596

The high accumulation rates at the two locations are primarily the result of the fast flowing WBUC. There is a possibility of fine sediment supply by ice-rafting during

the early Holocene (~7,800 years) at MD2024, as coarse lithic grains (characteristic of ice rafter debris) was found during this interval (Figure S1).

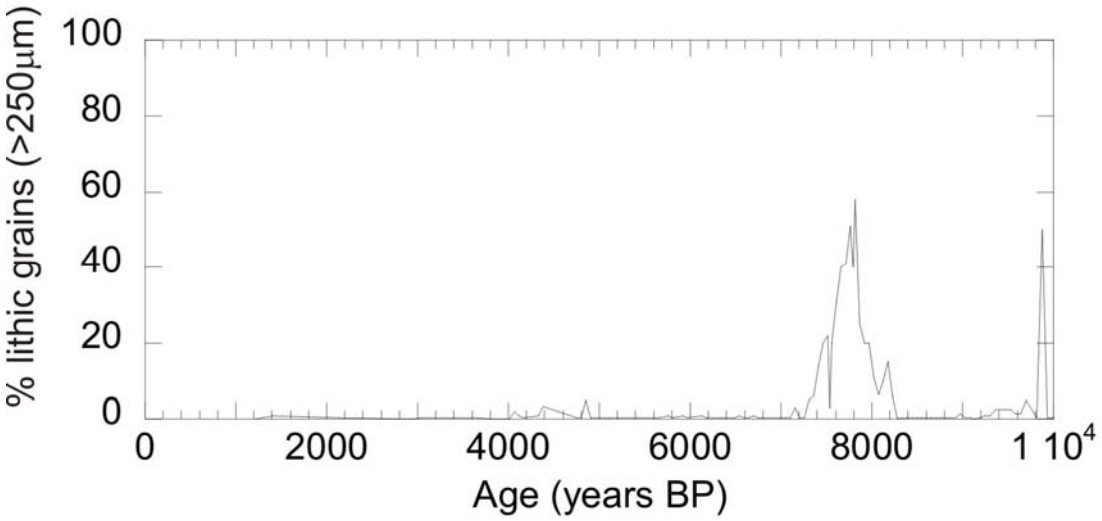

Figure S2: Percentage (100*lithic grains/total grains) coarse lithic grains from the > 250 µm fraction of core MD2024.

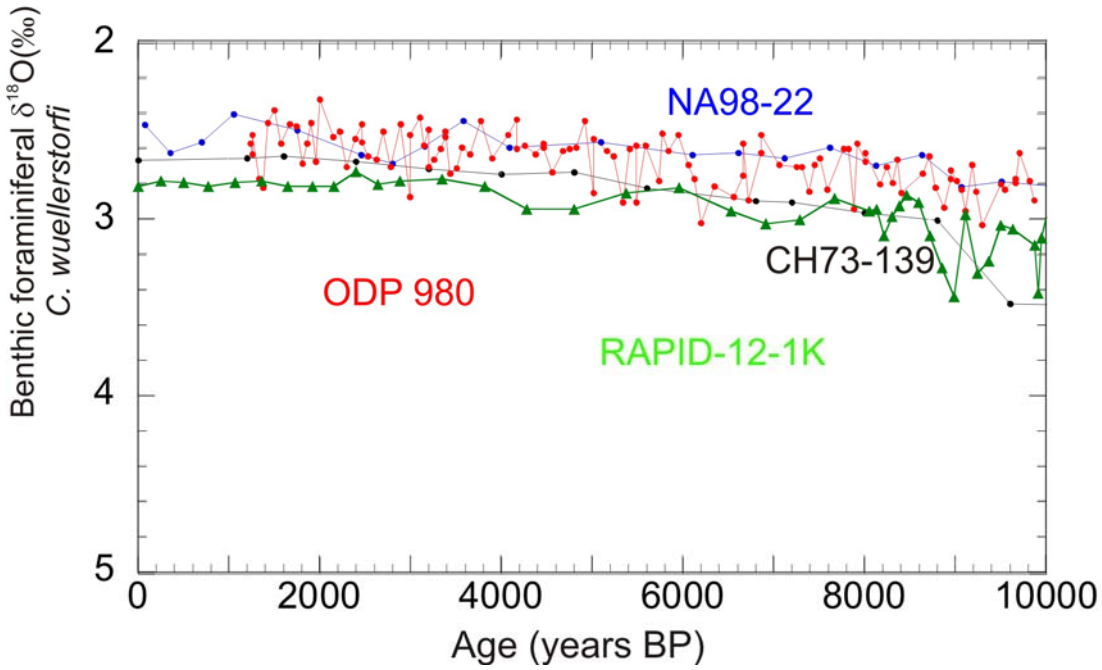

Figure S3: Additional low resolution benthic foraminiferal $\delta^{18}O_c$ records (all *C. wuellerstorfi*) NA98-22 (blue), CH73-139 (black) and RAPID-12-1K (green) (Curry et al., 1988; Duplessy et al., 1992; Thornally et al., 2010) from the northeast Atlantic also show a 0.2‰ decrease over the mid Holocene.

References

Curry, W. B., Duplessy, J. C., Labeyrie, L., Shackleton, N.J., 1988. Changes in the distribution of d13C of deep water SumCO2 between the last glaciation and the Holocene. Paleoceanography, 3, 317-341.

Duplessy, J.C., Labeyrie, L., Arnold, M., Paterne, M., Duprat, J., van Weering, T.C.E., 1992. Changes in surface salinity of the North Atlantic Ocean during the last deglaciation. Nature 358, 485-487.

Ellison, C.R.W., Chapman, M.R., Hall, I.R., 2006. Surface and deep ocean interactions during the cold climate event 8200 years ago. Science 312, 1929-1932.

Kleiven, H.F., Kissel, C., Laj, C., Ninnemann, U.S., Richter, T.O., Cortijo, E., 2008. Reduced North Atlantic Deep Water coeval with the glacial Lake Agassiz freshwater outburst. Science 319, 60-64.

Oppo, D.W., McManus, J.F., Cullen, J.L., 2003. Deepwater variability in the Holocene epoch. Nature 422, 277-278.

Sarnthein, M., van Kreveld, S., Erlenkeuser, H., Grootes, P.M., Kucera, M., Pflaumann, U., Schultz, M., 2003. Centennial-to-millennial-scale periodicities of Holocene climate and sediment injections off the western Barents shelf, 75°N. Boreas 32, 447-461.

Stuiver, M., Reimer, P.J., 1993. Extended 14C data base and revised CALIB 3.0 14C Age calibration program. Radiocarbon 35, 215-230.

Thornally, D.J.R., Elderfield, H., McCave, I.N., 2010. Intermediate and deep water paleoceanography of the northern North Atlantic over the past 21,000 years. Paleoceanography 25, doi:10.1019/2009PA001833.